Determining V_{tb} at Electron-Positron Colliders

Qing-Hong Cao[1,2,3,*] and Bin Yan[1,†]

[1] *Department of Physics and State Key Laboratory of Nuclear Physics and Technology, Peking University, Beijing 100871, China*

[2] *Collaborative Innovation Center of Quantum Matter, Beijing, China*

[3] *Center for High Energy Physics, Peking University, Beijing 100871, China*

arXiv:1507.06204v2 [hep-ph] 28 Nov 2015

Abstract

Verifying $V_{tb} \simeq 1$ is critical to test the three generation assumption of the Standard Model. So far our best knowledge of V_{tb} is inferred either from the 3×3 unitarity of CKM matrix or from single top-quark productions upon the assumption of universal weak couplings. The unitarity could be relaxed in new physics models with extra heavy quarks and the universality of weak couplings could also be broken if the Wtb coupling is modified in new physics models. In this work we propose to measure V_{tb} in the process of $e^+e^- \to t\bar{t}$ without prior knowledge of the number of fermion generations or the strength of the Wtb coupling. Using an effective Lagrangian approach, we perform a model-independent analysis of the interactions among electroweak gauge bosons and the third generation quarks, i.e. the Wtb, $Zt\bar{t}$ and $Zb\bar{b}$ couplings. The electroweak symmetry of the Standard Model specifies a pattern of deviations of the Z-t_L-t_L and W-t_L-b_L couplings after one imposes the known experimental constraint on the Z-b_L-b_L coupling. We demonstrate that, making use of the predicted pattern and the accurate measurements of top-quark mass and width from the energy threshold scan experiments, one can determine V_{tb} from the cross section and the forward-backward asymmetry of top-quark pair production at an *unpolarized* electron-positron collider.

*Electronic address: qinghongcao@pku.edu.cn

†Electronic address: binyan@pku.edu.cn

I. INTRODUCTION

The Cabibbo-Kobayashi-Maskawa (CKM) matrix element V_{tb} is an important parameter in the standard model (SM) of particle physics and remains untested directly. Measuring the V_{tb} accurately is important to test the unitarity of the CKM matrix and the assumption of three generations of fermions. The value of V_{tb} could be modified in many new physics (NP) models involving extra heavy quarks [1–8]. It is difficult to directly measure V_{tb} experimentally. Our knowledge of V_{tb} is obtained at hadron colliders either from the branching ratio of the top-quark decay into Wb mode in the top-quark pair production or through measuring the single top-quark production cross sections. However, some specific assumptions have to be made in order to extract out V_{tb} in both measurements.

In the first method, the top-quark decay branching ratio of the Wb mode is

$$R = \frac{\mathrm{Br}(t \to Wb)}{\sum_{q=d,s,b} \mathrm{Br}(t \to Wq)} \simeq \frac{|V_{tb}|^2}{\sum_{q=d,s,b} |V_{tq}|^2} = V_{tb}^2, \tag{1}$$

where the $SU(2)$ coupling g cancel out in both numerator and denominator. In the last step one has to use the unitarity condition of the CKM matrix, $\sum_{q=d,s,b} |V_{tq}|^2 = 1$, which implicitly assumes that three and only three generations of quarks exist in the nature. A very high precision of $|V_{tb}| = 0.99914 \pm 0.00005$, is derived directly from low energy precision data under the unitarity assumption of the 3×3 CKM matrix [9].

In the second method, the single top-quark production cross sections are proportional to weak gauge coupling g and V_{tb} as $\sigma_t \sim g^2 V_{tb}^2$. The limit on V_{tb} can be derived under assumption of $g = g_{Wtb}^{SM}$. The ATLAS and CMS collaborations report $|V_{tb}| = 0.97^{+0.09}_{-0.10}$ and $|V_{tb}| = 0.998 \pm 0.038$ (exp.) $\pm$ 0.016 (theo.), respectively [10, 11]. The gauge coupling of the Wtb interaction is different from the SM prediction in several NP models, e.g. the ununified [12–16] and top-flavor models [14–19]. In those models the third generation fermions are involved in a new gauge interaction. In such a case, one cannot link σ_t with V_{tb} directly. A precise knowledge of V_{tb} will help us to extract out the gauge coupling g from a precision measurement of the Wtb coupling $g_{Wtb} \sim gV_{tb}$ and vice versa. It thus offers an opportunity to verify the universality of the weak gauge coupling of SM. Observing a deviation in the gauge couplings from the SM prediction would shed light on various NP models.

Measuring V_{tb} without prior knowledge of the number of fermion generations or the $SU(2)$ coupling g is critical in NP searches. At an e^+e^- collider with a center of mass

energy $\sqrt{s} = 500$ GeV, $t\bar{t}$ pairs would be copiously produced, with several 100,000 events for an integrated luminosity of 500 fb^{-1} [20]. Such a large dataset offers a great opportunity of testing top-quark properties. In this work we perform a model-independent analysis of the gauge interaction of the third generation quarks. We argue that one could determine the V_{tb} from the precision measurements of the top-quark pair production at an *unpolarized* e^+e^- collider with $\sqrt{s} \sim 350 - 1000$GeV. Furthermore, we show that the measurement of V_{tb} is not sensitive to the collider energy in our method and $\sqrt{s} = 500$ GeV is enough to measure V_{tb} at percentage level.

II. EFFECTIVE GAUGE COUPLINGS

So far no heavy resonances are observed at the LHC yet. It is reasonable to assume the NP effects modify the SM theory prediction slightly and can be described by a set of higher dimensional operators made out of the SM fields [21],

$$\mathcal{L}_{\text{eff}} = \mathcal{L}_{\text{SM}} + \frac{1}{\Lambda^2}\sum_i (c_i \mathcal{O}_i + h.c.) + \mathcal{O}\left(\frac{1}{\Lambda^3}\right), \tag{2}$$

where $\mathcal{L}_{\text{SM}}$ denotes the Lagrangian of the SM, Λ is the characteristic scale of NP, $\mathcal{O}_i$ is the dimension-6 operator which satisfies the $SU(3)_c \otimes SU(2)_L \otimes U(1)_Y$ gauge symmetry, and c_i is Wilson coefficient which represents the strength of the operator $\mathcal{O}_i$. In this work, we consider those operators affecting top-quark gauge couplings and restrict ourselves to the interference between the SM and the operators when computing the effects of NP operators. Since the left-handed top quark and bottom quark form a $SU(2)_L$ weak doublet, the W-t_L-b_L coupling is always related to the Z-t_L-t_L and Z-b_L-b_L couplings [22]. It is, therefore, reasonable to combine the tree-level induced effective operators which are related to those couplings to determine V_{tb}, [1]

$$\begin{aligned}
\mathcal{O}_{\phi q}^{(1)} &= i\left(\phi^\dagger D_\mu \phi\right)\left(\bar{q}\gamma^\mu q\right), & \mathcal{O}_{\phi q}^{(3)} &= i\left(\phi^\dagger \tau^I D_\mu \phi\right)\left(\bar{q}\gamma^\mu \tau^I q\right), \\
\mathcal{O}_{\phi t} &= i\left(\phi^\dagger D_\mu \phi\right)\left(\bar{t}_R\gamma^\mu t_R\right), & \mathcal{O}_{\phi b} &= i\left(\phi^\dagger D_\mu \phi\right)\left(\bar{b}_R\gamma^\mu b_R\right), \\
\mathcal{O}_{\phi\phi} &= i\left(\tilde{\phi}^\dagger D_\mu \phi\right)\left(\bar{t}_R\gamma^\mu b_R\right), & &
\end{aligned} \tag{3}$$

where $D_\mu = \partial_\mu - ig(\tau^I/2)W_\mu^I - ig'YB_\mu$ is the gauge-covariant derivative, g and g' are the gauge couplings of $SU(2)_L$ and $U(1)_Y$, respectively, and Y is the hypercharge of the field

[1] The loop induced operators are usually suppressed by $1/(16\pi^2)$ and not considered in our analysis.

to which D_μ is applied, τ^I is the usual Pauli matrix; $q^T = (t_L,\, b_L)$ is the left-handed top-bottom $SU(2)_L$ doublet; $t_R(b_R)$ are corresponding to the right-handed isosinglets; and ϕ is $SU(2)_L$ weak doublet of Higgs field, defined as $\phi^T = 1/\sqrt{2}\ (0, v+h)$ with $v = 246$ GeV in the unitarity gauge with $\tilde{\phi} = i\tau^2\phi^*$. After symmetry breaking $\langle\phi\rangle = v/\sqrt{2}$, the set of operators generates the following corrections to the couplings Wtb, $Zt\bar{t}$ and $Zb\bar{b}$ [22–25],

$$\mathcal{O}_{Wtb} = \frac{c_{\phi q}^{(3)} v^2}{\Lambda^2}\frac{g}{\sqrt{2}} W_\mu^+ \bar{t}_L \gamma^\mu b_L + \frac{c_{\phi\phi} v^2}{2\Lambda^2}\frac{g}{\sqrt{2}} W_\mu^+ \bar{t}_R \gamma^\mu b_R + h.c., \tag{4}$$

$$\mathcal{O}_{Zt\bar{t}} = \frac{\left(c_{\phi q}^{(3)} - c_{\phi q}^{(1)}\right) v^2}{\Lambda^2}\frac{g}{2c_W} Z_\mu \bar{t}_L \gamma^\mu t_L - \frac{c_{\phi t} v^2}{\Lambda^2}\frac{g}{2c_W} Z_\mu \bar{t}_R \gamma^\mu t_R, \tag{5}$$

$$\mathcal{O}_{Zb\bar{b}} = -\frac{\left(c_{\phi q}^{(1)} + c_{\phi q}^{(3)}\right) v^2}{\Lambda^2}\frac{g}{2c_W} Z_\mu \bar{b}_L \gamma^\mu b_L - \frac{c_{\phi b} v^2}{\Lambda^2}\frac{g}{2c_W} Z_\mu \bar{b}_R \gamma^\mu b_R, \tag{6}$$

where $c_W \equiv \cos\theta_W$ is the cosine of the weak mixing angle.

The anomalous coupling $\mathcal{G}_R \equiv c_{\phi\phi} v^2/(2\Lambda^2)$ in the Wtb coupling, as severely constrained by the $b \to s\gamma$ data [26, 27], is within the window of $-8 \times 10^{-4} \leq \mathcal{G}_R \leq 2.1 \times 10^{-3}$. Furthermore, the LEP precision measurements require a strong cancellation between the two operators $\mathcal{O}_{\phi q}^{(1)}$ and $\mathcal{O}_{\phi q}^{(3)}$, i.e. $c_{\phi q}^{(1)} + c_{\phi q}^{(3)} \simeq 0$, which leaves the SM Z-b_L-b_L coupling unmodified [28]. It immediately enforces a correlation among the deviations of W-t_L-b_L coupling and Z-t_L-t_L coupling as follows:

$$\begin{aligned} g_{Wtb}^{\rm NP} &= (\Delta V_{tb} + \mathcal{F}_L)\frac{g}{\sqrt{2}} W_\mu^+ \bar{t}_L \gamma^\mu b_L + h.c., \\ g_{Ztt}^{\rm NP} &= 2\mathcal{F}_L \frac{g}{2c_W} Z_\mu \bar{t}_L \gamma^\mu t_L + \mathcal{F}_R \frac{g}{2c_W} Z_\mu \bar{t}_R \gamma^\mu t_R, \end{aligned} \tag{7}$$

where ΔV_{tb} is the deviation of the V_{tb} matrix element from the SM value $V_{tb}^0 = 1$, $\mathcal{F}_L = c_{\phi q}^{(3)} v^2/\Lambda^2$ and $\mathcal{F}_R = -c_{\phi t} v^2/\Lambda^2$. We assume the three coefficients are real in our calculation. Throughout this work $\Delta X \equiv X - X^0$ represents the deviation of the central value of variable X from the theory prediction X^0 and δX denotes the experimental error of X. Notice the relation between the coefficients of the left-handed neutral and charged currents [22, 29, 30],

$$(g_{Ztt}^{\rm NP})_L = 2\mathcal{F}_L = 2(g_{Wtb}^{\rm NP})_L - 2\Delta V_{tb}. \tag{8}$$

The relation holds for any underlying theory with an approximate custodial symmetry such that the vertex Z-b_L-b_L is not modified as discussed above [29]. It is possible to yield such a twice factor from an additional symmetry, e.g. certain subgroups of the custodial symmetry which protect the ρ parameter [31] and the Z-b_L-b_L coupling [32].

Recently, measuring Wtb anomalous couplings at the Large Hadron Collider (LHC) with recent experimental data are studied in Refs. [27, 33–36], which shows $-0.06 \leq \Delta V_{tb} + \mathcal{F}_L \leq 0.03$ at 95% confidence level. The $Zt\bar{t}$ coupling can be measured from the associated production of the top-quark pair and Z-boson. It is shown in Ref. [37] that $-0.99 \leq \mathcal{F}_L \leq 0.57$ at 95% confidence level at the 13 TeV LHC with 300 fb^{-1}. To further constrain the $\mathcal{F}_L$ at the LHC, it demands a fairly large luminosity to achieve a good precision. It is impossible to obtain an accurate V_{tb} from the Wtb and $Zt\bar{t}$ measurement at the LHC. The electron-positron collider provides a great opportunity to precisely determine both $\mathcal{F}_L$ and V_{tb} in the top-quark pair production.

III. PRECISIONS AT THE e^+e^- COLLIDER

A. Top-quark width measurement

At the e^+e^- collider the Wtb coupling can be extracted out from the top-quark width (Γ_t) measurements around the threshold region of a pair of top quarks [38]. In the SM the top-quark entirely decays into a bottom-quark and a W-boson. A state-of-art calculation of the top-quark decay width at next-to-next-to-leading order in quantum chromodynamics, including next-to-leading order electroweak correction and finite bottom quark mass and W boson width effect, is carried out recently in Ref. [39], which shows the top-quark width in the SM is

$$\Gamma_t^0 \equiv \Gamma_t^{\rm NNLO} = 0.8926 \times \Gamma_t^{\rm LO}, \tag{9}$$

where $\Gamma_t^{\rm LO}$ labels the top-quark decay width at the leading order in the limit of $m_{b,s,d} \to 0$,

$$\Gamma_t^{\rm LO} = \frac{G_F m_t^3}{8\sqrt{2}\pi} \sum_{i=d,s,b} |V_{ti}|^2 \left(1 - \frac{m_W^2}{m_t^2}\right)^2 \left(1 + \frac{2m_W^2}{m_t^2}\right). \tag{10}$$

Here, m_t denotes the top-quark mass, m_W is the W-boson mass and $G_F = 1.166 \times 10^{-5}{\rm GeV}^{-2}$ [9]. Using the branching ratio measurement,

$${\rm Br}(t \to Wb) = \frac{\Gamma(t \to Wb)}{\sum_{i=d,s,b} \Gamma(t \to Wi)} = \frac{|V_{tb}|^2}{\sum_{i=d,s,b} |V_{ti}|^2}, \tag{11}$$

we obtain

$$\Gamma_t^{\rm LO} = \frac{G_F m_t^3}{8\sqrt{2}\pi} \frac{|V_{tb}|^2}{{\rm Br}(t \to Wb)} \left(1 - \frac{m_W^2}{m_t^2}\right)^2 \left(1 + \frac{2m_W^2}{m_t^2}\right). \tag{12}$$

Here, we assume $\mathrm{Br}(t \to Wb)$ is the same as the SM prediction. Deviations of g, m_t and V_{tb} from the SM values modify the top-quark width as following

$$\frac{\Delta\Gamma_t}{\Gamma_t^0} = 3\frac{\Delta m_t}{m_t} + 2\Delta V_{tb} + 2\mathcal{F}_L, \tag{13}$$

where $\Delta\Gamma_t \equiv \Gamma_t - \Gamma_t^0$. Both m_t and Γ_t can be measured precisely from the threshold scan at the e^+e^- collider with $\sqrt{s} = 340 - 350$ GeV. It is shown that m_t and Γ_t could be measured with an accuracy of 0.006% and 0.5%, respectively [40]. Thus, we ignore the small deviation of the top quark mass and assume the error $\delta\Gamma_t/\Gamma_t^0 \simeq 0.01$ hereafter. Under such a circumstance ΔV_{tb} depends mainly on the precision measurement of $\mathcal{F}_L$,

$$\Delta V_{tb} \simeq \frac{1}{2}\frac{\Delta\Gamma_t}{\Gamma_t^0} - \mathcal{F}_L. \tag{14}$$

One then can determine the V_{tb} if the $\mathcal{F}_L$ could be measured precisely. However, it is difficult to measure $\mathcal{F}_L$ from the Z-boson and top-quark pair associated production ($pp \to Zt\bar{t}$) at the LHC [37, 41, 42]. On the other hand, $\mathcal{F}_L$ could be well measured at a e^+e^- collider through the process of $e^+e^- \to \gamma/Z \to t\bar{t}$ [20, 43–46]. In this study we focus on unpolarized electron and positron beams.

B. Top-quark pair production

The anomalous couplings of $\mathcal{F}_L$ and $\mathcal{F}_R$ can be measured from the inclusive cross section of $t\bar{t}$ pair produciton ($\sigma_{t\bar{t}}$) and the forward-backward asymmetry of top quarks (A_{FB}), which is defined as

$$A_{FB} \equiv \frac{\sigma_F - \sigma_B}{\sigma_F + \sigma_B}, \tag{15}$$

where

$$\sigma_F = \int_0^1 \frac{d\sigma}{d\cos\theta_t} d\cos\theta_t \ , \ \sigma_B = \int_{-1}^0 \frac{d\sigma}{d\cos\theta_t} d\cos\theta_t. \tag{16}$$

with θ_t being the polar angle of top-quark inside the center-of-mass frame. A simple algebra shows

$$\begin{aligned} \sigma_{t\bar{t}} &= \sigma_{t\bar{t}}^0 \left(1 + a_L\mathcal{F}_L + a_R\mathcal{F}_R\right), \\ A_{FB} &= A_{FB}^0 \left(1 + b_L\mathcal{F}_L + b_R\mathcal{F}_R\right). \end{aligned} \tag{17}$$

Here $\sigma_{t\bar{t}}^0$ and A_{FB}^0 are the cross section of top quark pair and the forward and backward asymmetry of top quarks in the SM, respectively. The coefficients $a_{L/R}$ and $b_{L/R}$ describe

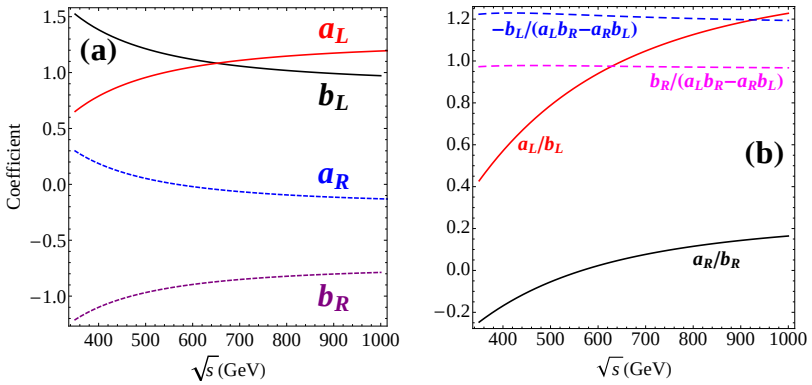

FIG. 1: *Dependence on the collider energy $\sqrt{s}$: (a) the coefficients and (b) the ratios.*

the interference effects between the SM and anomalous couplings. The detailed expressions of $a_{L/R}$ and $b_{L/R}$ are given in the Appendix. It is straightforward to determine $\mathcal{F}_L$ and $\mathcal{F}_R$ from $\sigma_{t\bar{t}}$ and A_{FB} as follows:

$$\mathcal{F}_L = \frac{b_R}{a_L b_R - a_R b_L}\left(\frac{\Delta\sigma_{t\bar{t}}}{\sigma^0_{t\bar{t}}} - \frac{a_R}{b_R}\frac{\Delta A_{FB}}{A^0_{FB}}\right), \tag{18}$$

$$\mathcal{F}_R = \frac{-b_L}{a_L b_R - a_R b_L}\left(\frac{\Delta\sigma_{t\bar{t}}}{\sigma^0_{t\bar{t}}} - \frac{a_L}{b_L}\frac{\Delta A_{FB}}{A^0_{FB}}\right), \tag{19}$$

where $\Delta\sigma_{t\bar{t}} \equiv (\sigma_{t\bar{t}} - \sigma^0_{t\bar{t}})$ and $\Delta A_{FB} \equiv (A_{FB} - A^0_{FB})$.

The values of the coefficients of a_L, a_R, b_L and b_R depend on the collider energy ($\sqrt{s}$). Figure 1(a) displays those coefficients as a function of the collider energy $\sqrt{s}$. Various ratios of those coefficients are also plotted in Fig. 1(b), which shows $b_R/(a_Lb_R - a_Rb_L) \sim 0.97$ and $-b_L/(a_Lb_R - a_Rb_L) \sim 1.21$. As a result, Eqs. 18 and 19 can be approximated as follows:

$$\mathcal{F}_L \sim 0.97\left(\frac{\Delta\sigma_{t\bar{t}}}{\sigma^0_{t\bar{t}}} - \frac{a_R}{b_R}\frac{\Delta A_{FB}}{A^0_{FB}}\right) \sim 0.97\frac{\Delta\sigma_{t\bar{t}}}{\sigma^0_{t\bar{t}}}, \tag{20}$$

$$\mathcal{F}_R \sim 1.21\left(\frac{\Delta\sigma_{t\bar{t}}}{\sigma^0_{t\bar{t}}} - \frac{a_L}{b_L}\frac{\Delta A_{FB}}{A^0_{FB}}\right), \tag{21}$$

where we ignore the a_R/b_R term in the second step as $|a_R/b_R| \lesssim 0.2$ in the region of 400 GeV $\leq \sqrt{s} \leq$ 1000 GeV. The ratio a_L/b_L varies from 0.4 to 1.2 in the same energy regime. Note that the above approximation serves only as a guide line for understanding the dependence of $\mathcal{F}_{L/R}$ on $\sigma_{t\bar{t}}$ and A_{FB}. In practice one has to combine the measurements of both $\sigma_{t\bar{t}}$ and A_{FB} in order to determine $\mathcal{F}_L$ accurately.

Obviously, $\mathcal{F}_L$ depends mainly on the cross section measurement. We plot in Fig. 2 the contour of $\mathcal{F}_R$ in the plane of $\Delta\sigma_{t\bar{t}}/\sigma^0_{t\bar{t}}$ and $\Delta A_{FB}/A^0_{FB}$ for three collider energies: (a)

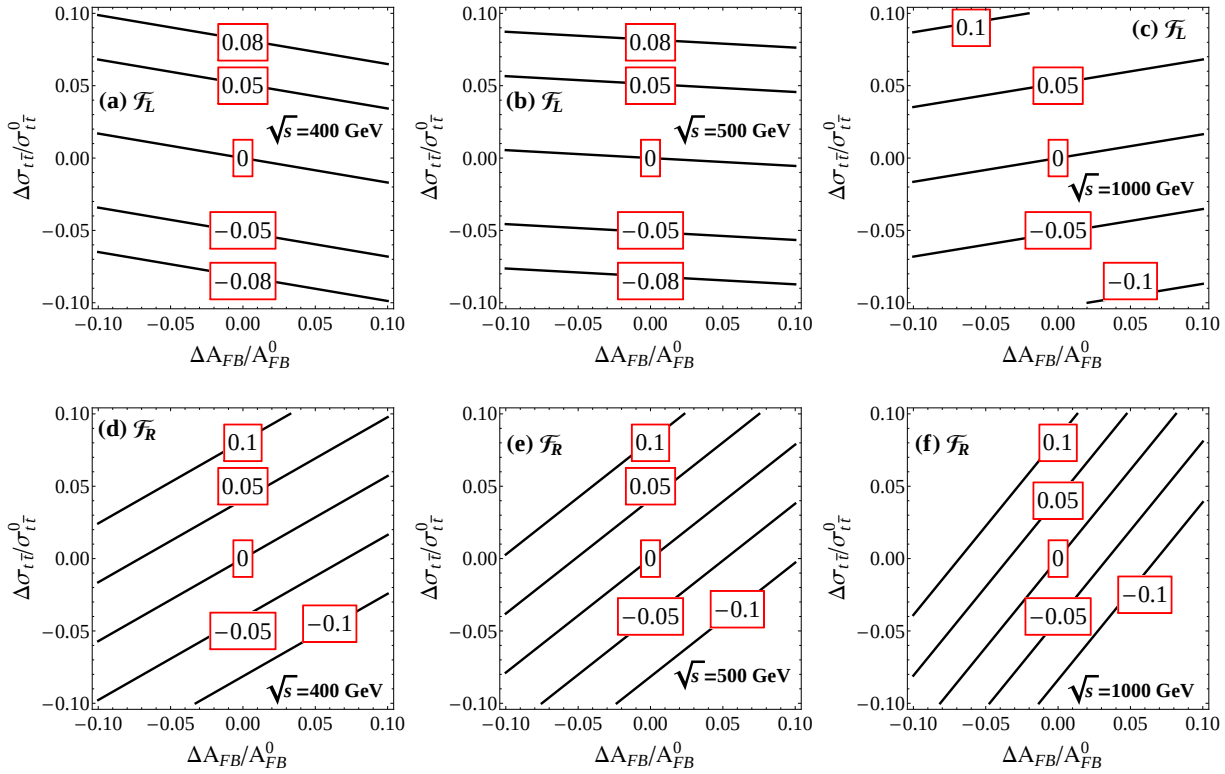

FIG. 2: *The contours of $\mathcal{F}_{L/R}$ in the plane of $\Delta\sigma_{t\bar{t}}/\sigma^0_{t\bar{t}}$ and $\Delta A_{FB}/A^0_{FB}$ for $\sqrt{s}$ =400, 500 and 1000 GeV.*

$\sqrt{s} = 400$ GeV, (b) 500 GeV and (c) 1000 GeV. The slope of the contour lines is determined only by the ratio a_R/b_R; see Eq. 18. The difference of $\mathcal{F}_L$ contour lines at $\sqrt{s} = 400$ GeV and 1000 GeV can be easily understood from the a_R/b_R curve shown in Fig. 1(b), which shows $a_R/b_R < 0$ for $\sqrt{s} < 566$ GeV and $a_R/b_R > 0$ for $\sqrt{s} > 566$ GeV.

The determination of $\mathcal{F}_R$ relies on both $\sigma_{t\bar{t}}$ and A_{FB} measurements. We also plot the contours of $\mathcal{F}_{L/R}$ in the plane of $\Delta\sigma_{t\bar{t}}/\sigma^0_{t\bar{t}}$ and $\Delta A_{FB}/A^0_{FB}$ in Fig. 2 (d, e, f) for the three collider energies. Again, the slope of $\mathcal{F}_R$ contour lines depends on the ratio of a_L/b_L: see Eq. 19. Since the ratio a_L/b_L is always positive for 400 GeV $\leq \sqrt{s} \leq$ 1000 GeV, the $\mathcal{F}_R$ contours are very similar for the three collider energies.

There is a strong anti-correlation between ΔV_{tb} and $\Delta\sigma_{t\bar{t}}$ as

$$\Delta V_{tb} \approx \frac{1}{2}\frac{\Delta\Gamma_t}{\Gamma^0_t} - 0.97\frac{\Delta\sigma_{t\bar{t}}}{\sigma^0_{t\bar{t}}}. \tag{22}$$

For simplicity we assume $\Delta\Gamma_t \simeq 0$, i.e. the top-quark width is exactly the same as the SM theory prediction. Figure 3 displays the contour of $V_{tb} \equiv 1 + \Delta V_{tb}$ in the plane of

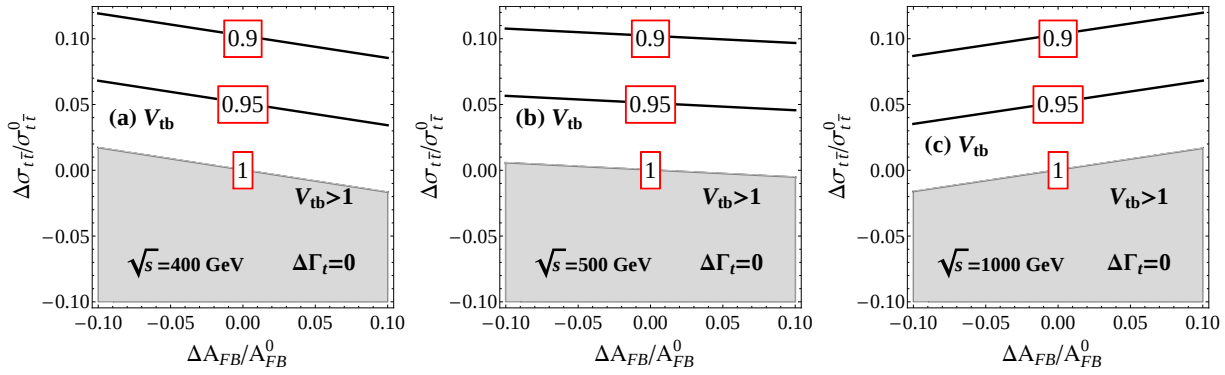

FIG. 3: *The contours of* V_{tb} *in the plane of* $\Delta\sigma_{t\bar{t}}/\sigma^0_{t\bar{t}}$ *and* $\Delta A_{FB}/A^0_{FB}$ *for* $\sqrt{s}$ *=400, 500 and 1000 GeV under the assumption of* $\Delta\Gamma_t \simeq 0$. *The gray shaded region represents the parameter space of* $V_{tb} > 1$.

$\Delta\sigma_{t\bar{t}}/\sigma^0_{t\bar{t}}$ and $\Delta A_{FB}/A^0_{FB}$. The shaded region represents $V_{tb} > 1$ (i.e. $\Delta V_{tb} > 0$) which violates the unitarity condition. Demanding $V_{tb} \leq 1$ in NP models implies that $\sigma_{t\bar{t}}$ would be likely enhanced. In order to precisely determine the value of V_{tb} matrix element, both measurements of $\sigma_{t\bar{t}}$ and A_{FB} are needed. However, we emphasize that, at an *unpolarized* e^+e^- collider with $\sqrt{s} = 500$ GeV, the measurement of $\sigma_{t\bar{t}}$ alone is already good to probe $\mathcal{F}_L$ which can be used to determine ΔV_{tb}. For example, a 5% deviation in the $\sigma_{t\bar{t}}$ cross section indicates $V_{tb} \simeq 0.95$, regardless of the A_{FB} measurement.

C. Error analysis

Next we discuss the uncertainties of extracting $\mathcal{F}_L$ and $\mathcal{F}_R$ out of the cross section and asymmetry measurements. Based on the error propagation equation of the weighted-sum functions, the errors of $\mathcal{F}_L$ and $\mathcal{F}_R$ are,

$$\begin{aligned}
\delta\mathcal{F}_L &= \left|\frac{b_R}{a_L b_R - a_R b_L}\right| \sqrt{\left(\frac{\delta\sigma_{t\bar{t}}}{\sigma^0_{t\bar{t}}}\right)^2 + \left(\frac{a_R}{b_R}\right)^2 \left(\frac{\delta A_{FB}}{A^0_{FB}}\right)^2}, \\
\delta\mathcal{F}_R &= \left|\frac{b_L}{a_L b_R - a_R b_L}\right| \sqrt{\left(\frac{\delta\sigma_{t\bar{t}}}{\sigma^0_{t\bar{t}}}\right)^2 + \left(\frac{a_L}{b_L}\right)^2 \left(\frac{\delta A_{FB}}{A^0_{FB}}\right)^2},
\end{aligned} \tag{23}$$

where $\delta\sigma_{t\bar{t}}$ and δA_{FB} denote the total errors of the $\sigma_{t\bar{t}}$ and A_{FB} defined as follows:

$$\delta\sigma_{t\bar{t}} \equiv \sqrt{(\delta\sigma_{t\bar{t}})^2_{sys.} + (\delta\sigma_{t\bar{t}})^2_{stat.}}, \qquad \delta A_{FB} \equiv \sqrt{(\delta A_{FB})^2_{sys.} + (\delta A_{FB})^2_{stat.}}. \tag{24}$$

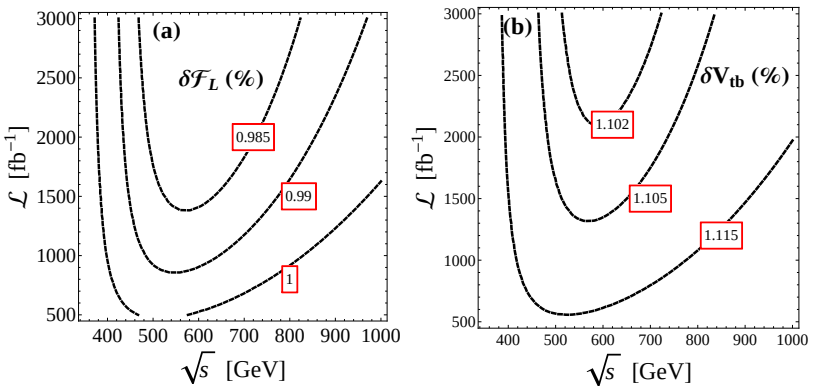

FIG. 4: *The contours of uncertainties of $\mathcal{F}_L$ and V_{tb} measurements denoted by $\delta\mathcal{F}_L$ and δV_{tb} in the plane of the collider energy $\sqrt{s}$ (GeV) and integrated luminosity $\mathcal{L}$ (fb^{-1}).*

The statistical errors of $\sigma_{t\bar{t}}$ and A_{FB}, which are normalized to the SM predictions, are

$$\begin{aligned}(\delta\sigma_{t\bar{t}}/\sigma^0_{t\bar{t}})_{stat.} &= \sqrt{1/(\mathcal{L}\sigma^0_{t\bar{t}})}\ , \\ (\delta A_{FB}/A^0_{FB})_{stat.} &= \sqrt{(1-(A^0_{FB})^2)/(\mathcal{L}\sigma^0_{t\bar{t}})}. \end{aligned} \tag{25}$$

For an integrated luminosity of 500 fb^{-1} and collider energy $\sqrt{s} = 500$ GeV, $(\delta\sigma_{t\bar{t}}/\sigma^0_{t\bar{t}})_{stat.} \simeq (\delta A_{FB}/A^0_{FB})_{stat.} \sim 0.002$.

The systematic uncertainty arises from a lot of experimental effects, e.g. cut acceptance, b-tagging efficiency, detector resolution, luminosity or different hadronization of $t\bar{t}$ events, etc. Those systematic uncertainties will have to be estimated at a later stage, but they are expected to be small [20]. The LEP-I reported a systematic uncertainty on R_b of 0.28 % [47] which may serve as a guide line for values to be expected at the future e^+e^- collider. In this work, the systematic error of $\sigma_{t\bar{t}}$ relative to the SM prediction is assumed to be around 1%, i.e. $(\delta\sigma_{t\bar{t}}/\sigma^0_{t\bar{t}})_{sys.} = 0.01$ [20, 43]. Table I displays the statistical and systematic errors of m_t, Γ_t, $\sigma_{t\bar{t}}$ and A_{FB} used in this study.

Figure 4(a) displays the contours of $\delta\mathcal{F}_L$ in the plane of the collider energy $\sqrt{s}$ (GeV) and integrated luminosity $\mathcal{L}$ (fb^{-1}). It shows that $\mathcal{F}_L$ can be measured with an accuracy of percentage, e.g. $\delta\mathcal{F}_L \leq 1\%$. The uncertainty, which is dominated by the systematic error, cannot be further improved by increasing the collider energy and accumulating more luminosities. One then can translate the uncertainty of $\mathcal{F}_L$ measurement to the V_{tb} measurement

TABLE I: The statistical and systematic uncertainties of m_t, Γ_t, $\sigma_{t\bar{t}}$ and A_{FB}. The statistic uncertainties of m_t and Γ_t are quoted from Ref. [40] while the statistical error of $\sigma_{t\bar{t}}$ and A_{FB} are obtained at a 500 GeV collider with an integrated luminosity of 500 fb^{-1}. The systematic error of Γ_t, $\sigma_{t\bar{t}}$ and A_{FB} are assumed to be $\sim 1\%$ throughout this work. The uncertainties of R_b measured at LEP-I are listed for reference [47].

	m_t	Γ_t	$\sigma_{t\bar{t}}$	A_{FB}	R_b (LEP-I)
stat.	0.006%	0.5%	0.2%	0.2%	0.44%
sys.	-	1%	1%	1%	0.28%

as following

$$\delta V_{tb} = \sqrt{\frac{1}{4}\left(\frac{\delta\Gamma_t}{\Gamma_t^0}\right)^2 + (\delta F_L)^2}\ . \tag{26}$$

Figure 4(b) displays that δV_{tb} can be measured as accurately as $\delta\mathcal{F}_L$, e.g. $\delta V_{tb} \leq 1.1\%$, and it is not sensitive to the collider energy or the integrated luminosities. Therefore, we argue that it is enough to determine V_{tb} at the e^+e^- collider with $\sqrt{s} \gtrsim 400$ GeV. We also note that the cross section measurement alone is adequate to determine $\mathcal{F}_L$ when $\sqrt{s} \geq 500$ GeV. To further constrain the δV_{tb}, it is necessary to reduce the systematic error and improve the measurement of top quark width.

IV. IMPLICATIONS ON NEW PHYSICS MODELS

For illustration we examine the impact of the V_{tb} and $\mathcal{F}_{L,R}$ measurements on NP models. We begin with the so-called fourth-generation model [1–8]. The perturbative fourth generation is disfavored as it would induce a large gluon-gluon-Higgs effective coupling which produces a too large cross section of the Higgs boson production to obey the current data [6–8]. However, vector-like quarks, which exhibit the decoupling behavior, would not affect the Higgs production too much if the vector-like quarks are very heavy. The vector-quarks might modify the CKM matrix elements, depending on their quantum number. It is critical to directly measure the V_{tb} element which is complementary to the H-g-g coupling measurement. Next we use the fourth-generation model as a good example to discuss the impact of V_{tb} measurement. Our results can be extended easily to NP models with extra heavy quarks which modify V_{tb} through the mixing of the heavy quarks and the third generation quarks.

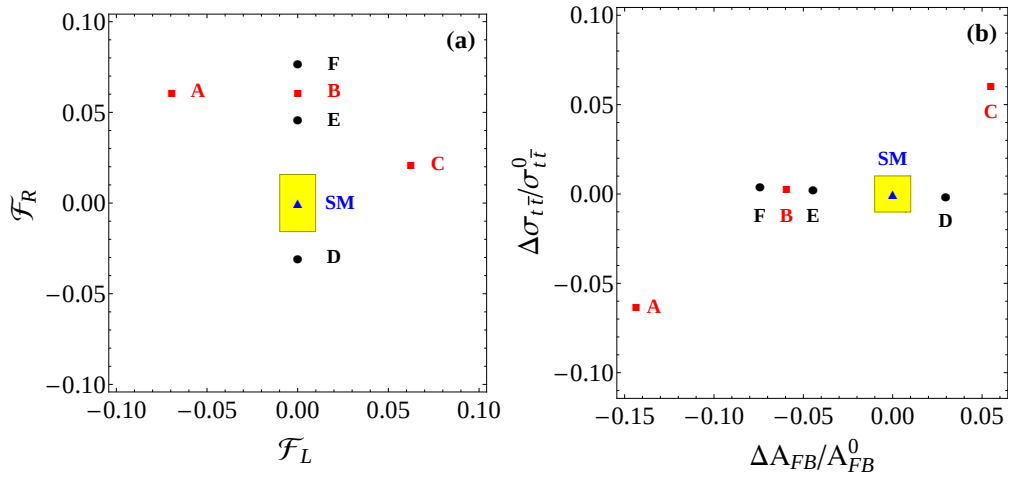

FIG. 5: *Projected 68.3% C.L. bounds (shaded yellow region) on (a) the anomalous $Zt\bar{t}$ copulings and (b) $\sigma_{t\bar{t}}$ and A_{FB} measurements at a 500 GeV e^+e^- collider with an integrated luminosity of* 500 fb^{-1}. *Several benchmark points of NP models are also shown: the red box denotes the extra dimensional models: A (Gherghetta et al [48]), B (Carena et al [49]), C (Hostanoi et al [50]), the black disk denotes the composite models: D (Grojean et al [51]), E (Little Higgs [52]), F (Pomarol et al [53]).*

Neglecting the possible CP-violating phases beyond 3×3 CKM matrix $V_{3\times3}$, we can parametrize the 4×4 unitary matrix $V_{4\times4}$ with $V_{3\times3}$ and extra mixing angles as follows [4],

$$V_{4\times4} = R_{34}(\theta_{34})R_{24}(\theta_{24})R_{14}(\theta_{14}) \begin{pmatrix} V^0_{3\times3} & \mathbf{1}_{1\times3} \\ \mathbf{1}_{3\times1} & 1 \end{pmatrix}, \tag{27}$$

where $V^0_{3\times3}$ denote the CKM matrix involving the three generation fermions in the SM, $R_{ij}(\theta_{ij})$ is the rotation matrix in the (i, j) flavour plane with rotation angle θ_{ij}. Since $V^0_{tb} \gg V^0_{cb,ub}$ in $V^0_{3\times3}$, one can approximate the V_{tb} matrix element as

$$V_{tb} \equiv V^0_{tb} + \Delta V_{tb} \approx \cos\theta_{34} V^0_{tb} = \cos\theta_{34}. \tag{28}$$

Thus, the dependence of $\cos\theta_{34}$ on the $\sigma_{t\bar{t}}$ and A_{FB} measurements is exactly the same as those of V_{tb} shown in Fig. 3. The uncertainties on $\cos\theta_{34}$ are also identical to those in Fig. 4(b).

A by-product of measuring V_{tb} in the process of $e^+e^- \to t\bar{t}$ is to determine both $\mathcal{F}_L$ and $\mathcal{F}_R$ precisely, which can be used to distinguish different NP models. The $Zt\bar{t}$ couplings could be modified in various NP models, e.g. the extra dimension models [48–50], composite

models [51–53] and non-Abelian extension models [14–16]. Several benchmark points of those NP models mentioned above are nicely summarized in Table I of Ref. [54]. Figure 5(a) displays the expected precision of the $\mathcal{F}_L$ and $\mathcal{F}_R$ measurements and the benchmark points of NP models at an unpolarized e^+e^- collider with $\sqrt{s} = 500$ GeV and $\mathcal{L} = 500$ fb^{-1}. The shaded region denotes the expected uncertainties based on the error analysis discussed above. The triangle symbol represents the SM, the black disk denotes the composite model while the red box the extra dimension models. For $\sqrt{s} = 500$ GeV, the $\mathcal{F}_L$ and $\mathcal{F}_R$ anomalous couplings are related to $\sigma_{t\bar{t}}$ and A_{FB} as follows:

$$\mathcal{F}_L = 0.98\frac{\Delta\sigma_{t\bar{t}}}{\sigma^0_{t\bar{t}}} - 0.05\frac{\Delta A_{FB}}{A^0_{FB}}, \quad \mathcal{F}_R = 1.23\frac{\Delta\sigma_{t\bar{t}}}{\sigma^0_{t\bar{t}}} - 0.97\frac{\Delta A_{FB}}{A^0_{FB}}.$$

Figure 5(b) displays the NP models in the plane of $\Delta\sigma_{t\bar{t}}/\sigma^0_{t\bar{t}}$ and $\Delta A_{FB}/A^0_{FB}$. Those NP models can be easily discriminated if they modify the $Zt\bar{t}$ anomalous couplings sizably.

V. SUMMARY

In this work we proposed to measure the V_{tb} element of the CKM matrix in the process of $e^+e^- \to t\bar{t}$ without assuming the 3×3 unitarity of CKM matrix and universality of weak gauge couplings. Four experimental observables are considered in our analysis: the top-quark mass and width, the cross section of top-quark pair production $\sigma_{t\bar{t}}$, and the Forward-Backward asymmetry of the top-quark A_{FB}. We first consider the impact of NP effects on the top-quark mass and width which can be measured very precisely from the threshold energy scan experiments at e^+e^- colliders. The would-be measured top-quark width imposes a strong correlation between the deviation of V_{tb} (denoted by ΔV_{tb}) and the deviation of W-t_L-b_L coupling (denoted by $\mathcal{F}_L$). In order to determine V_{tb}, $\mathcal{F}_L$ must be measured from other sources. Using an effective Lagrangian approach, we perform a model-independent analysis of the interactions among electroweak gauge bosons and the third generation quarks, i.e. the Wtb, $Zt\bar{t}$ and $Zb\bar{b}$ couplings. After one imposes the known experimental constraint on the Z-b_L-b_L coupling, the electroweak $SU(2)_L \times U(1)_Y$ symmetry of the SM specifies a pattern of deviations of the Z-t_L-t_L and W-t_L-b_L couplings, independent of underlying new physics scenarios. The predicted pattern enables us to infer $\mathcal{F}_L$ from the $Zt\bar{t}$ coupling measurement in the process of $e^+e^- \to t\bar{t}$ at an unpolarized e^+e^- collider.

The deviations of the $Zt\bar{t}$ coupling are described by the left-handed coupling $\mathcal{F}_L$ and

right-handed coupling $\mathcal{F}_R$, which can be determined from $\sigma_{t\bar{t}}$ and A_{FB}. We show that $\mathcal{F}_L$ relies mainly on $\Delta\sigma_{t\bar{t}}$ at an unpolarized e^+e^- collider, especially for $\sqrt{s} \geq 500$ GeV. It leads to a strong anti-linear correlation between ΔV_{tb} and $\Delta\sigma_{t\bar{t}}$, $\Delta V_{tb} \approx 0.5\Delta\Gamma_t/\Gamma_t^0 - 0.97\Delta\sigma_{t\bar{t}}/\sigma_{t\bar{t}}^0$, where Γ_t^0 and $\sigma_{t\bar{t}}^0$ denote the top-quark width and the cross section of top-quark pair production, respectively. If the top-quark width is not modified in NP models, requiring $V_{tb} < 1$ (i.e. $\Delta V_{tb} \leq 0$) implies that $\sigma_{t\bar{t}}$ will be inevitably enhanced. We also show that the uncertainty of V_{tb} measurement is dominated by the systematic errors which is assumed to be 1% in this work.

On the other hand, $\mathcal{F}_R$ is sensitive to the deviations of both $\sigma_{t\bar{t}}$ and A_{FB}. One has to combine $\sigma_{t\bar{t}}$ and A_{FB} to obtain a precise value of $\mathcal{F}_R$. Knowing both $\mathcal{F}_L$ and $\mathcal{F}_R$ is important to distinguish new physics models.

Acknowledgments

We thank Yan-Dong Liu, C.-P. Yuan and Chen Zhang for helpful discussions. The work is supported in part by the National Science Foundation of China under Grand No. 11275009.

Appendix A: The $\sigma_{t\bar{t}}$ and A_{FB} at a e^+e^- collider

The cross section $\sigma_{t\bar{t}}$ and the asymmetry A_{FB} of top-quark pairs in the process $e^+e^- \to \gamma/Z \to t\bar{t}$ are given as follows:

$$\begin{aligned}
\sigma_{t\bar{t}} &= \sigma_{t\bar{t}}^0 \left(1 + a_L\mathcal{F}_L + a_R\mathcal{F}_R\right) = \sigma_{t\bar{t}}^0 \left(1 + a_V F_V + a_A F_A\right), \\
A_{FB} &= A_{FB}^0 \left(1 + b_L\mathcal{F}_L + b_R\mathcal{F}_R\right) = A_{FB}^0 \left(1 + b_V F_V + b_A F_A\right),
\end{aligned} \tag{A1}$$

where

$$\begin{aligned}
F_V &= (\mathcal{F}_L + \mathcal{F}_R/2)/2, & F_A &= (-\mathcal{F}_L + \mathcal{F}_R/2)/2, \\
a_V &= a_L + 2a_R, & a_A &= 2a_R - a_L, \\
b_V &= b_L + 2b_R, & b_A &= 2b_R - b_L.
\end{aligned} \tag{A2}$$

The $\sigma^0_{t\bar{t}}$ and A^0_{FB} denote the cross section and asymmetry in the SM, respectively, and are given as follows:

$$\begin{aligned}
\sigma^0_{t\bar{t}} &= \frac{\beta(3-\beta^2)s}{8\pi}\left(G^V_{\gamma\gamma}+2G^V_{Z\gamma}+G^V_{ZZ}+\frac{2\beta^2}{3-\beta^2}G^A_{ZZ}\right), \\
A^0_{FB} &= \frac{-3\beta(H_{\gamma Z}+2H_{ZZ})}{(3-\beta^2)(G^V_{\gamma\gamma}+2G^V_{Z\gamma}+G^V_{ZZ})+2\beta^2 G^A_{ZZ}},
\end{aligned} \tag{A3}$$

with β being the velocity of the top quark in the center-of-mass frame. The $G^{V,A}_{X,Y}$ and $H_{X,Y}$ factors are

$$\begin{aligned}
G^{V,A}_{X,Y} &= \frac{g_e(X,Y)g^t_{V,A}(X)g^t_{V,A}(Y)}{(s-m^2_X)\,(s-m^2_Y)}, \\
H_{X,Y} &= \frac{g^e_V(X)g^t_V(X)g^e_A(Y)g^t_A(Y)}{(s-m^2_X)\,(s-m^2_Y)},
\end{aligned} \tag{A4}$$

where

$$g_e(X,Y) = \begin{cases} g^e_V(\gamma)^2, & X=Y=\gamma, \\ g^e_V(\gamma)g^e_V(Z), & X=\gamma, Y=Z, \\ g^e_V(Z)^2+g^e_A(Z)^2, & X=Y=Z. \end{cases} \tag{A5}$$

Here, $g^i_{V,A}(X/Y)$ denotes the vector (V) and axial-vector (A) coupling of gauge boson $X/Y = \gamma, Z$ to the electron ($i=e$) and top quark ($i=t$). In the SM,

$$\begin{aligned}
g^i_A(\gamma) &= 0, & g^i_V(\gamma) &= Q_i g s_W, \\
g^i_A(Z) &= \frac{g}{c_W}g^i_A, & g^i_V(Z) &= \frac{g}{c_W}g^i_V,
\end{aligned} \tag{A6}$$

where Q_i is the electric charge of fermion i, $g^i_A = -T^i_3/2$ and $g^i_V = T^i_3/2 - Q_i s^2_W$ with $T^e_3 = -1/2$ and $T^t_3 = 1/2$, $s_W \equiv \sin\theta_W$ is the sine of the weak mixing angle. The coefficients a_V, a_A, b_V and b_A are

$$\begin{aligned}
a_V &= \frac{2(G^V_{Z\gamma}+G^V_{ZZ})}{g^t_V\left[G^V_{\gamma\gamma}+2G^V_{Z\gamma}+G^V_{ZZ}+2\beta^2/(3-\beta^2)G^A_{ZZ}\right]}, \\
a_A &= \frac{4\beta^2 G^A_{ZZ}}{g^t_A\left[(3-\beta^2)(G^V_{\gamma\gamma}+2G^V_{Z\gamma}+G^V_{ZZ})+2\beta^2 G^A_{ZZ}\right]}, \\
b_V &= \frac{2H_{ZZ}}{g^t_V\left[H_{\gamma Z}+2H_{ZZ}\right]} - a_V, \\
b_A &= \frac{1}{g^t_A} - a_A.
\end{aligned} \tag{A7}$$

The explicit expresses of $a_{L/R}$ and $b_{L/R}$ can be obtained from $a_{V/A}$ and $b_{V/A}$ as follows:

$$\begin{aligned}
a_L &= \frac{1}{\left[G^V_{\gamma\gamma}+2G^V_{Z\gamma}+G^V_{ZZ}+2\beta^2/(3-\beta^2)G^A_{ZZ}\right]}\Big(\frac{G^V_{Z\gamma}+G^V_{ZZ}}{g^t_V}-\frac{2\beta^2 G^A_{ZZ}}{g^t_A(3-\beta^2)}\Big),\\
a_R &= \frac{1}{2\left[G^V_{\gamma\gamma}+2G^V_{Z\gamma}+G^V_{ZZ}+2\beta^2/(3-\beta^2)G^A_{ZZ}\right]}\Big(\frac{G^V_{Z\gamma}+G^V_{ZZ}}{g^t_V}+\frac{2\beta^2 G^A_{ZZ}}{g^t_A(3-\beta^2)}\Big),\\
b_L &= \frac{1}{2}\Big(\frac{2H_{ZZ}}{g^t_V\left[H_{\gamma Z}+2H_{ZZ}\right]}-\frac{1}{g^t_A}\Big)-a_L,\\
b_R &= \frac{1}{4}\Big(\frac{2H_{ZZ}}{g^t_V\left[H_{\gamma Z}+2H_{ZZ}\right]}+\frac{1}{g^t_A}\Big)-a_R.
\end{aligned} \tag{A8}$$

[1] S. Bose and E. A. Paschos, Nucl.Phys. **B169**, 384 (1980).

[2] M. Gronau and J. Schechter, Phys.Rev. **D31**, 1668 (1985).

[3] F. Botella and L.-L. Chau, Phys.Lett. **B168**, 97 (1986).

[4] J. Alwall, R. Frederix, J.-M. Gerard, A. Giammanco, M. Herquet, et al., Eur.Phys.J. **C49**, 791 (2007), hep-ph/0607115.

[5] G. D. Kribs, T. Plehn, M. Spannowsky, and T. M. Tait, Phys.Rev. **D76**, 075016 (2007), 0706.3718.

[6] E. Kuflik, Y. Nir, and T. Volansky, Phys.Rev.Lett. **110**, 091801 (2013), 1204.1975.

[7] O. Eberhardt, G. Herbert, H. Lacker, A. Lenz, A. Menzel, et al., Phys.Rev.Lett. **109**, 241802 (2012), 1209.1101.

[8] O. Eberhardt, A. Lenz, A. Menzel, U. Nierste, and M. Wiebusch, Phys.Rev. **D86**, 074014 (2012), 1207.0438.

[9] K. Olive et al. (Particle Data Group), Chin.Phys. **C38**, 090001 (2014).

[10] T. A. collaboration (ATLAS) (2014).

[11] V. Khachatryan et al. (CMS), JHEP **1406**, 090 (2014), 1403.7366.

[12] H. Georgi, E. E. Jenkins, and E. H. Simmons, Phys.Rev.Lett. **62**, 2789 (1989).

[13] H. Georgi, E. E. Jenkins, and E. H. Simmons, Nucl.Phys. **B331**, 541 (1990).

[14] K. Hsieh, K. Schmitz, J.-H. Yu, and C.-P. Yuan, Phys.Rev. **D82**, 035011 (2010), 1003.3482.

[15] Q.-H. Cao, Z. Li, J.-H. Yu, and C. Yuan, Phys.Rev. **D86**, 095010 (2012), 1205.3769.

[16] Q.-H. Cao, B. Yan, and D.-M. Zhang (2015), 1507.00268.

[17] X. Li and E. Ma, Phys.Rev.Lett. **47**, 1788 (1981).

[18] E. Malkawi, T. M. Tait, and C. Yuan, Phys.Lett. **B385**, 304 (1996), hep-ph/9603349.

[19] H.-J. He, T. M. Tait, and C. Yuan, Phys.Rev. **D62**, 011702 (2000), hep-ph/9911266.

[20] M. Amjad, M. Boronat, T. Frisson, I. Garcia, R. Poschl, et al. (2013), 1307.8102.

[21] W. Buchmuller and D. Wyler, Nucl.Phys. **B268**, 621 (1986).

[22] E. L. Berger, Q.-H. Cao, and I. Low, Phys.Rev. **D80**, 074020 (2009), 0907.2191.

[23] J. M. Yang and B.-L. Young, Phys.Rev. **D56**, 5907 (1997), hep-ph/9703463.

[24] K. Whisnant, J.-M. Yang, B.-L. Young, and X. Zhang, Phys.Rev. **D56**, 467 (1997), hep-ph/9702305.

[25] J. Aguilar-Saavedra, Nucl.Phys. **B812**, 181 (2009), 0811.3842.

[26] B. Grzadkowski and M. Misiak, Phys.Rev. **D78**, 077501 (2008), 0802.1413.

[27] Q.-H. Cao, B. Yan, J.-H. Yu, and C. Zhang (2015), 1504.03785.

[28] J. Abdallah et al. (DELPHI), Eur.Phys.J. **C60**, 1 (2009), 0901.4461.

[29] E. Malkawi and C. P. Yuan, Phys. Rev. **D50**, 4462 (1994), hep-ph/9405322.

[30] D. O. Carlson, E. Malkawi, and C. P. Yuan, Phys. Lett. **B337**, 145 (1994), hep-ph/9405277.

[31] P. Sikivie, L. Susskind, M. B. Voloshin, and V. I. Zakharov, Nucl. Phys. **B173**, 189 (1980).

[32] K. Agashe, R. Contino, L. Da Rold, and A. Pomarol, Phys.Lett. **B641**, 62 (2006), hep-ph/0605341.

[33] C.-R. Chen, F. Larios, and C. P. Yuan, Phys. Lett. **B631**, 126 (2005), [AIP Conf. Proc.792,591(2005)], hep-ph/0503040.

[34] Q.-H. Cao, J. Wudka, and C. P. Yuan, Phys. Lett. **B658**, 50 (2007), 0704.2809.

[35] M. Fabbrichesi, M. Pinamonti, and A. Tonero, Eur. Phys. J. **C74**, 3193 (2014), 1406.5393.

[36] C. Bernardo, N. F. Castro, M. C. N. Fiolhais, H. Gonalves, A. G. C. Guerra, M. Oliveira, and A. Onofre, Phys. Rev. **D90**, 113007 (2014), 1408.7063.

[37] R. Rntsch and M. Schulze, JHEP **1407**, 091 (2014), 1404.1005.

[38] T. Horiguchi, A. Ishikawa, T. Suehara, K. Fujii, Y. Sumino, et al. (2013), 1310.0563.

[39] J. Gao, C. S. Li, and H. X. Zhu, Phys.Rev.Lett. **110**, 042001 (2013), 1210.2808.

[40] M. Bicer et al. (TLEP Design Study Working Group), JHEP **1401**, 164 (2014), 1308.6176.

[41] U. Baur, A. Juste, L. Orr, and D. Rainwater, Phys.Rev. **D71**, 054013 (2005), hep-ph/0412021.

[42] U. Baur, A. Juste, D. Rainwater, and L. Orr, Phys.Rev. **D73**, 034016 (2006), hep-ph/0512262.

[43] H. Baer, T. Barklow, K. Fujii, Y. Gao, A. Hoang, et al. (2013), 1306.6352.

[44] D. Asner, A. Hoang, Y. Kiyo, R. Pschl, Y. Sumino, et al. (2013), 1307.8265.

[45] D. Barducci, S. De Curtis, S. Moretti, and G. M. Pruna (2015), 1504.05407.

[46] M. Amjad, S. Bilokin, M. Boronat, P. Doublet, T. Frisson, et al. (2015), 1505.06020.

[47] S. Schael et al. (SLD Electroweak Group, DELPHI, ALEPH, SLD, SLD Heavy Flavour Group, OPAL, LEP Electroweak Working Group, L3), Phys. Rept. **427**, 257 (2006), hep-ex/0509008.

[48] Y. Cui, T. Gherghetta, and J. Stokes, JHEP **1012**, 075 (2010), 1006.3322.

[49] M. Carena, E. Ponton, J. Santiago, and C. E. Wagner, Nucl.Phys. **B759**, 202 (2006), hep-ph/0607106.

[50] Y. Hosotani and M. Mabe, Phys.Lett. **B615**, 257 (2005), hep-ph/0503020.

[51] C. Grojean, O. Matsedonskyi, and G. Panico, JHEP **1310**, 160 (2013), 1306.4655.

[52] C. Berger, M. Perelstein, and F. Petriello (2005), hep-ph/0512053.

[53] A. Pomarol and J. Serra, Phys.Rev. **D78**, 074026 (2008), 0806.3247.

[54] F. Richard (2014), 1403.2893.